International Information and Engineering Technology Association
Advancing the World of Information and Engineering

Mathematical Modelling of Engineering Problems
Vol. 9, No. 6, December, 2022, pp. 1596-1602
Journal homepage: http://iieta.org/journals/mmep

Similarity Investigation of Thermosolutal Mixed Convection in a Saturated Porous Medium

Mohamed El Haroui[1], El Yazid Flilihi[2*], Driss Achemlal[2], Mohammed Sriti[3]

[1] Faculty of Sciences and Techniques, Mechanics, Energy Efficiency and Renewable Energy Laboratory (L.M.3.E.R), Moulay Ismail University, Boutalamine, Errachidia B.P. 509, Morocco
[2] Polydisciplinary Faculty of Taza, Engineering Sciences Laboratory, Sidi Mohamed Ben Abdellah University, Taza B.P. 1223, Morocco
[3] Department of Energy, ENSAM Engineering School, Moulay Ismail University, Al Mansour, Meknes B.P. 15290, Morocco

Corresponding Author Email: elyazid_flilihi@yahoo.fr

https://doi.org/10.18280/mmep.090620

Received: 30 June 2022
Accepted: 3 October 2022

Keywords:
thermosolutal, mixed convection, porous medium, non-uniform permeability, suction /injection

ABSTRACT

This contribution investigates the thermosolutal convection phenomenon around a thin wall, vertically immersed in a fluid saturating a porous medium of non-uniform permeability, taking into account the thermal conditions of the wall which is exposed to a fluid suction/injection. The conservation equations with boundary conditions have been transformed by the similarity method into a set of nonlinear differential equations. The resulting equations are numerically resolved using a fifth-order Runge-Kutta scheme coupled with the shooting technique. A graphical and physical interpretation of the found results as a function of the control parameters was performed. It is noticed that the heat transfer rate and the mass transfer rate at wall, are intensified for free convection and for significant permeability.

1. INTRODUCTION

Thermosolutal convection is the phenomenon of fluid flow caused by the coupled influences of thermal and concentration gradients. Due to many important industrial and environmental applications including geothermal and petroleum recovery, contaminant transport in saturated soils, moisture migration in fibrous insulation, and others, thermosolutal convection in porous media has aroused significant interest from academic researchers and concerned organizations. Extensive theoretical, numerical, and experimental studies on the phenomenon of double diffusive convection in media porous are detailed in the works carried out by Nield and Bejan [1], Ingham and Pop [2, 3] and Vafai [4].

An experimental study of doubly diffusive free convection in a saturated porous medium was first conducted by Murray and Chen [5]. The authors showed a good agreement between the experimental and theoretical results. Then, Postelnicu and Pop [6], Postelnicu et al. [7] and Achemlal et al. [8] used the similarity transformations to study free thermal convection through a vertical or horizontal planar wall inserted in a saturated porous medium, in the presence of variable heat source with suction/injection of fluid. The impacts of thermal radiation and inside heat source on thermal convection along a vertical thin wall, with non-uniform temperature, have been realized by Cortell [9] and recently by Flilihi et al. [10] who used the Darcy-Brinkman law with the convective term, by taking into account the orientation of the plate. Alhumoud [11] studied the conjugate free convective heat transfer behavior in an enclosure with two solid thick surfaces. The results show that increasing all of controlling parameters results in increasing the heat transfer in the cavity. Belhadj et al. [12] investigated both heat transfer and fluid flow in a cavity filled with porous media using Darcy Brinkman-Forcheimer formulation. The authors found that increasing Rayleigh and Darcy numbers resulted in enhancing the convective heat transfer rate, which decreases with increasing porosity of the medium. Anghel et al. [13], Postelnicu [14] and Alam and Rahman [15] have studied the Soret-Dufour conjugate influences on thermosolutal convection within a saturated porous medium. Furthermore, Postelnicu [16] and El Haroui et al. [17] considered the existence of a chemical reaction when studying double-diffusive convection through a vertical wall of variable temperature. The authors showed the reduction of the concentration boundary layer and the increase in the mass transfer rate at wall when the chemical reaction is significant.

Harfash and Meften [18] studied the influence of various flow controlling parameters on the stability of binary mixture in a fluid layer by using linear, nonlinear and weighted energy analysis. Recently, Mahajan and Tripathi [19] analysed the variable temperature and concentration gradient effects on the behavior of heat and mass transfer problems.

To our knowledge, in the works cited above and many others, the permeability of the medium is considered to be constant. However, experimental measurements made by Roblee et al. [20] and Benenati and Brosilow [21] show that permeability varies from the wall to the ambient medium. Mohammadein and El-Shaer [22] and Singh [23] introduced variable permeability to study thermal convection in porous media and they noted a crucial effect of permeability variation on velocity and temperature profiles.

This work is a numerical study of mixed thermosolutal convective flow caused by a heated wall, vertically immersed in a fluid saturating a porous medium with non-uniform permeability. The study carried out takes into account the thermal state of the wall, with a lateral fluid flow (suction/injection), and aims to show the evolution of the velocity, thermal and species concentration profiles near the wall and also to quantify the rates of heat and mass transfer for various controlling parameters.

2. MATHEMATICAL FORMULATION

In this work, we study the phenomenon of doubly diffusive convection, around a heated vertical permeable wall, embedded in a fluid saturated porous medium. Figure 1 shows the geometric model of the problem studied. The x and y coordinates are measured, respectively, along and normal to the wall. The temperature $T_w(x)$ of the wall surface is assumed to be variable, while its concentration C_w is maintained constant. The wall is subjected to a fluid suction/injection, which is proportional to $x^{(\lambda-1)/2}$ expression. Away from the wall, the reference values for temperature and concentration are, respectively, T_∞ and C_∞. As simplifying assumptions, we assume that the flow is laminar, permanent, and bidirectional, the local thermal equilibrium between the fluid and the porous medium is verified, the permeability of the porous medium does not depend on the wall temperature, the Darcy's law is valid and the fluid density varies according to the following Boussinesq approximation:

$$\rho=\rho_\infty(1-\beta_T(T-T_\infty)-\beta_c(C-C_\infty)) \tag{1}$$

where, β_T and β_c are, respectively, the thermal expansion coefficient and the concentration expansion coefficient, ρ_∞ is the reference fluid density away from the wall.

In this study, we consider low flow velocities and small permeability of the medium in order to reduce the Navier-Stokes equation to the Darcy model after calculations.

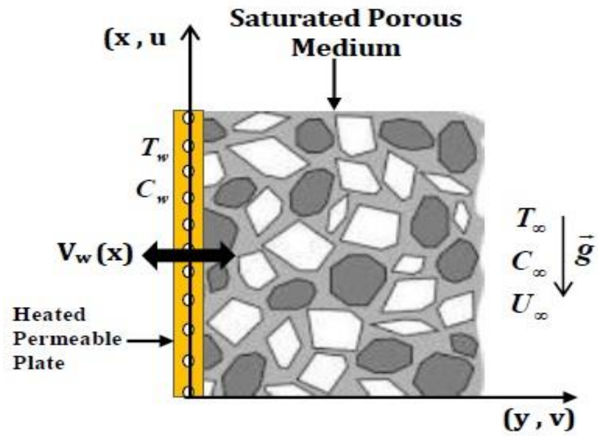

Figure 1. Physical configuration and coordinate system

By considering the above mentioned assumptions and the Boussinesq model for the fluid density, the conservation equations governing the studied phenomenon are given by:

$$\frac{\partial u}{\partial x}+\frac{\partial v}{\partial y}=0 \tag{2}$$

$$u=\frac{K(y)\,g}{\nu}(\beta_T(T-T_\infty)+\beta_c(T-T_\infty)) \tag{3}$$

$$u\frac{\partial T}{\partial x}+v\frac{\partial T}{\partial y}=a\frac{\partial^2 T}{\partial y^2} \tag{4}$$

$$u\frac{\partial C}{\partial x}+v\frac{\partial C}{\partial y}=D_M\frac{\partial^2 C}{\partial y^2}+D_T\frac{\partial^2 T}{\partial y^2} \tag{5}$$

This studied problem is governed by the following boundary conditions:

$$\begin{cases} x\geq 0, \quad y=0: \quad v=V_w(x),\ T=T_w(x),\ C=C_w \\ x\geq 0, \quad y\to\infty: u=U_\infty,\ T=T_\infty,\ C=C_\infty \end{cases} \tag{6}$$

Here u and v represent the Darcian velocity coordinates, T is the temperature of binary fluid, C is the species concentration, ν is the kinematic viscosity, a is the thermal diffusivity, ρ is the density of binary fluid, K is the permeability of the porous medium, g is the gravitational acceleration, D_T is the thermal diffusion coefficient and D_M is the mass diffusion coefficient.

The temperature $T_w(x)$ along the wall and the velocity fluid suction/injection across it $V_w(x)$ are, respectively, expressed as follows:

$$T_w(x)=T_\infty+Ax^\lambda \tag{7}$$

$$V_w(x)=Bx^{(\lambda-1)/2} \tag{8}$$

A and B are constants where λ is the temperature exponent charactering the thermal condition of the wall such as: $\lambda=1$ for linear temperature distribution along the wall, $\lambda=1/3$ for uniform heat flux through the wall and $\lambda=0$ for uniform temperature (isothermal wall).

We assume that the permeability of the medium fluctuates in the range of validity of Darcy's law according to the following model of Ress and Pop [22]:

$$K(y)=K_\infty+(K_w-K_\infty)e^{-\frac{y}{L}} \tag{9}$$

where, K_w is the permeability at wall, K_∞ is the permeability away from the wall (ambient medium) and L is the size of the area in which the permeability varies.

Due to coupling and non-linearity of equations, the direct analytical resolution of the mathematical model together with boundary conditions proves to be delicate. For this, we have adopted a semi-analytical method, called similarity, to convert the two-dimensional mathematical model of the problem into a model based on differential equations.

We then propose the following dimensionless variables:

$$\eta=\frac{y}{x}Ra_x^{\frac{1}{2}}, \quad \theta=\frac{T-T_\infty}{T_w-T_\infty}, \quad \phi=\frac{C-C_\infty}{C_w-C_\infty}, \quad \psi=a\,Ra_x^{\frac{1}{2}}f(\eta), \quad Ra_x=\frac{gK\beta_T(T_w-T_\infty)}{\nu a}x \tag{10}$$

where, η is the similarity variable, θ is the dimensionless temperature of the fluid in the boundary layer area, ϕ is the dimensionless species concentration of fluid in the boundary layer area, Ra_x is the local thermal Rayleigh number and ψ represents the stream function that satisfies the continuity Eq. (2) which is expressed by:

$$u = \frac{\partial \psi}{\partial y}, \quad v = -\frac{\partial \psi}{\partial x} \tag{11}$$

From $L = x.Ra_x^{-\frac{1}{2}}$ in Eq. (9), the non-dimensional permeability is purely function of η and given by:

$$K(\eta) = K_\infty (1 + (p-1)e^{-\eta}) \tag{12}$$

$p = \frac{K_w}{K_\infty}$ being the permeability parameter. Since porous media are, generally, packed near solid walls, we restrict attention to values of permeability parameter p which must be greater than 1 ($K_w > K_\infty$) and less than 10 (See [24]). For this, the permeability is uniform for $p=1$ and non-uniform in the case of $1<p<10$.

By injecting the transformations given by the system (10) into the Eqns. (3)-(5) and using the Boussinesq approximation, we find the following local similarity equations:

$$f' - \gamma - (1 + (p-1)e^{-\eta})(\theta + N\phi) = 0 \tag{13}$$

$$\theta'' + \frac{(\lambda+1)}{2} f\theta' - \lambda f'.\theta = 0 \tag{14}$$

$$\frac{1}{Le}\phi'' + \frac{(\lambda+1)}{2} f\phi' = 0 \tag{15}$$

With the boundary conditions:

$$\begin{cases} \eta = 0, \quad f = f_w, \; f' = \gamma + p(\theta + N\phi), \; \theta = 1, \; \phi = 1 \\ \eta \to \infty, \quad f' = \gamma, \; \theta = 0, \; \phi = 0 \end{cases} \tag{16}$$

where, f is the dimensionless stream function, $\gamma = \frac{Ra_x}{Pe_x}$ is the mixed convection parameter, $Pe_x = \frac{U_\infty x}{a}$ is the local peclet number, $U_\infty = \frac{g\beta_T K_\infty (T_W - T_\infty)}{\nu}$ corresponds to the uniform velocity away from the plate, N and Le are, respectively, buoyancy ratio number and Lewis number, $f_W = -2B\left(\frac{\nu}{ag\beta_T K(T_W - T_\infty)}\right)^{1/2}$ is the suction/injection parameter such as: $f_w>0$ for suction, $f_w<0$ in the case of injection and $f_w = 0$ for impermeable wall.

It is important to note that N and Le numbers are fixed at $N=1$ and $Le=1$. Their effects have already been discussed in our previous work [25].

The local heat flux q_T and the local mass flux q_m through the wall are expressed as:

$$q_T = -k\left(\frac{\partial T}{\partial y}\right)_{y=0} \tag{17}$$

$$q_m = -D_M\left(\frac{\partial C}{\partial y}\right)_{y=0} \tag{18}$$

The heat transfer rate and the mass transfer rate at the wall are expressed, respectively, by the local Nusselt number and the local Sherwood number. These two numbers are given by:

$$Nu_x = \frac{q_T x}{k} \tag{19}$$

$$Sh_x = \frac{q_m x}{D_M} \tag{20}$$

After calculation, we find their expressions in dimensionless form as follows:

$$Nu_x = -\theta'(0)\, Ra_x^{1/2} \tag{21}$$

$$Sh_x = -\phi'(0)\, Ra_x^{1/2} \tag{22}$$

3. NUMERICAL RESOLUTION PROCEDURE

The second-order nonlinear ordinary differential Eqns. (13), (14) and (15), coupled with the boundary conditions (Eq. (16)) are numerically solved using the fifth-order Runge-Kutta scheme associated with the shooting iteration technique. For various values of temperature exponent λ, the wall thermal and concentration gradients, consecutively, $\theta'(0)$ and $\phi'(0)$, are predicted and Eqns. (13) to (15) are integrated until the boundary conditions $f'(0)$, $\theta(0)$ and $\phi(0)$ are verified. Otherwise, the numerical process uses the calculated corrections to the estimated the values of $\theta'(0)$ and $\phi'(0)$ then iteratively repeated up to the boundary conditions $f'(\infty)$, $\theta(\infty)$ and $\phi(\infty)$ are satisfied. A uniform calculation step of $\Delta\eta = 10^{-3}$ is found adequate to ensure convergence with an error $\Delta\eta = 10^{-3}$.

4. RESULTS ANALYSIS

In this section, we present for various thermal states of the plate. the found numerical results in the form of figures, which illustrate the influence of suction/injection parameter f_w, mixed convection parameter γ and permeability parameter p on the wall heat and mass transfer rates that are represented by the local Nusselt number (Nu_x) and the local Sherwood number (Sh_x), respectively. However, only three values of λ representing physical solutions were considered: $\lambda=(0, 1/3, 1)$. As already mentioned, we distinguish between three cases for the suction/injection parameter: $f_w< 0$ for injection, $f_w> 0$ for suction and $f_w = 0$ for impermeable wall. The Regime transfer is characterized by the mixed convection parameter γ such that: $\gamma<1$ for forced convection regime, $\gamma=1$ for mixed convection regime and $\gamma>1$ for free convection regime.

To validate the computational code developed in the context of this paper, we present in Table 1 a comparison of our results with the previously published data in terms of the thermal gradient at the surface for various values of f_w at $p=1$ and $\gamma\to\infty$, when the plate is exposed to a uniform heat flux ($\lambda=1/3$). We note a good agreement which justified by a maximum relative error (RE) not exceeding 0.88%.

Table 1. Wall thermal gradient $-\theta'(0) = Nu_x Ra_x^{-1/2}$ for $\boldsymbol{\lambda = \frac{1}{3}, f_w \neq 0, p = 1\ and\ \gamma \to \infty}$

λ	f_w	Present results	Postelnicu et al. [7]	RE (%)	Cortell [9]	RE (%)
1/3	-1	- 0.0663	- 0.0662	0.15	-0.066178	0.18
	- 0.6	- 0.00944	- 0.0094	0.42	- 0.009357	0.88
	0.6	0.2877	0.2869	0.28	0.286887	0.28
	1	0.4288	0.4289	0.02	0.428891	0.02

Figure 2 presents dimensionless velocity profiles in the boundary layer area over an isothermal and impermeable plate at $p=2$ and various values of γ. It is very remarkable here; that the velocity profiles are amplified while passing from the forced convection regime to the free convection regime. This shows that the free convection promotes the fluid flow near the plate in comparison with forced convection. This can be justified by the influence of the high permeability near the plate which favors more the flow in the boundary layer area and by the effect of the imposed flow velocity away from the plate. We also note a stabilization of the velocity at an equilibrium state far from the plate ($f'(\infty)=\gamma$).

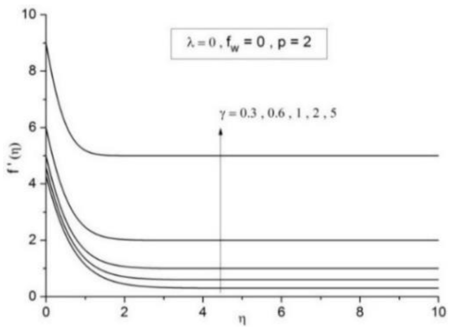

Figure 2. Velocity profiles at $\lambda=0, f_w=0, p=2$ and various values of γ

Figure 3 shows for $\gamma=1$, the effect of permeability parameter p on dimensionless velocity evolution in the boundary layer thickness of an impermeable plate subject to a linear distribution of the temperature ($\lambda = 1$). Here, it is clearly seen that the flow is important near the surface when the porous medium is more permeable ($K_w > K_\infty$) in comparison with the case where the permeability is uniform ($K_w = K_\infty$). Outside the boundary layer area, the flow is no sensitive to the permeability parameter variation. It is therefore concluded that the high permeability in the dynamic boundary layer promotes the flow compared to the case of a uniform permeability. In addition, for all selected values of p, the velocity profiles tend to an equilibrium state which is controlled by the boundary condition ($f'(\infty)=\gamma$).

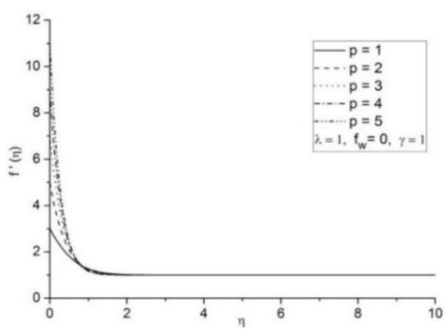

Figure 3. Velocity profiles at $\lambda=1, f_w=0, \gamma=1$ and various values of p

Figure 4 illustrates the dimensionless temperature profiles in the thermal boundary layer along an isothermal and impermeable plate for $p=2$ and different values of mixed convection parameter γ. Here, the thermal profiles are more amplified in the case of forced convection regime ($\gamma < 1$) and are reduced for free regime convection. Physically, the increase in buoyancy forces for free convection generates significant flow velocities, which leads to the rapid cooling observed all near the wall, leading to a reduction of the thermal boundary layer thickness. It can also be concluded that the dominance of the forced convection regime in the mixture promotes the heat transfer in the thermal boundary layer area, unlike the free convection which leads to the evacuate it.

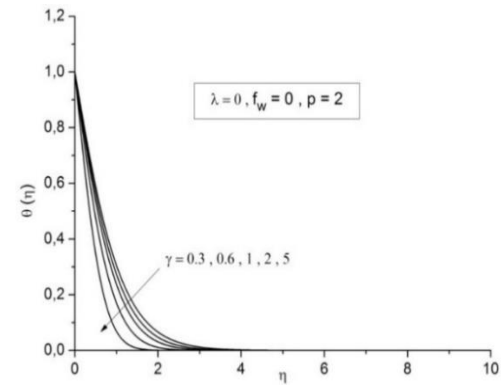

Figure 4. Temperature profiles at $\lambda=0, f_w=0, p=2$ and various values of γ

The effect of the permeability parameter p, for $\gamma = 1$, on dimensionless thermal profiles of an impermeable plate subjected to a linear distribution of the temperature ($\lambda = 1$) is presented in Figure 5. We notice that increasing the permeability of the porous medium near to the surface reduce the thermal boundary layer thickness. Therefore, the high permeability allows the evacuation of heat in the boundary layer area.

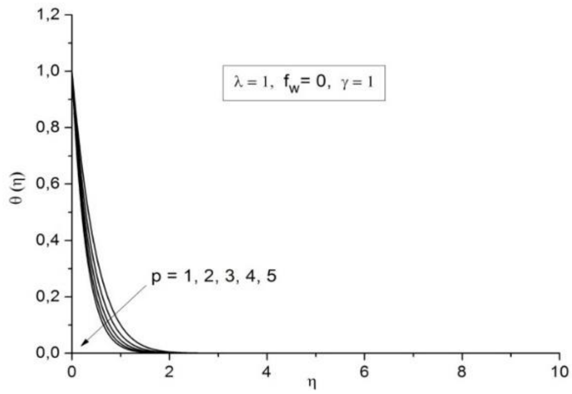

Figure 5. Temperature profiles at $\lambda=1, f_w=0, \gamma=1$, and various values of p

In Figure 6 we illustrate over an isothermal and impermeable plate, the dimensionless concentration profiles for $p=2$ and various values of γ. It is notable that the forced convection ($\gamma<1$) amplifies the profiles concentration, while the free convection reduces them. This can be explained by the effect of buoyancy forces generating significant flow velocities when forced convection regime is dominant, which leads to a rapid solute transfer near the plate and therefore a reduction in the concentration boundary layer thickness, unlike the case of the free convection regime dominance.

The effect of the permeability parameter p, for $\gamma=1$, on dimensionless concentration profiles in the boundary layer area of an impermeable plate at $\lambda=1$ is shown in Figure 7. Form this graph, we observe that increasing the permeability of porous medium near the surface, makes it possible to reduce the concentration boundary layer thickness.

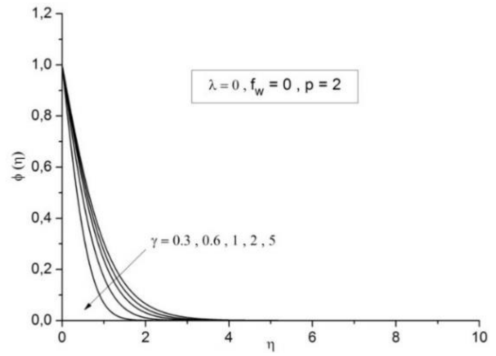

Figure 6. Concentration profiles at $\lambda=0, f_w=0, p=2$ and various values of γ

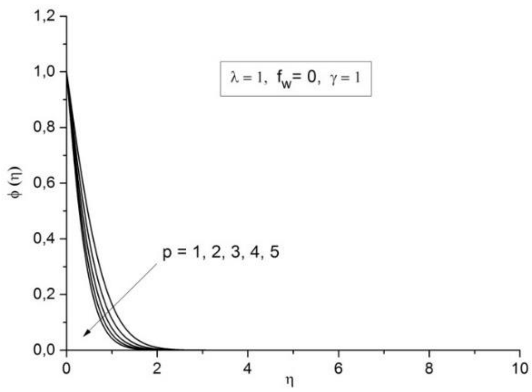

Figure 7. Concentration profiles at $\lambda=1, f_w=0, \gamma=1$ and various values of p

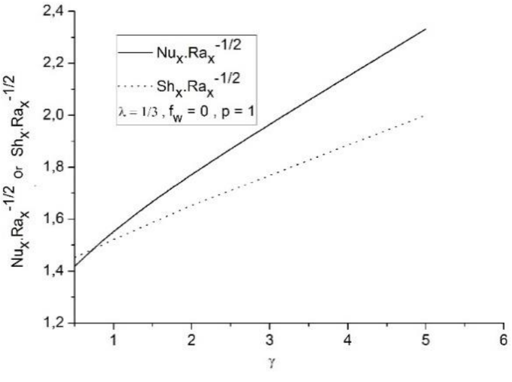

Figure 8. Nu_x and Sh_x distributions versus γ at $\lambda=1/3, f_w=0$ and $p=1$

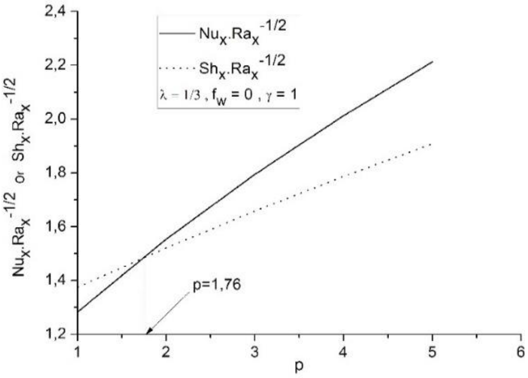

Figure 9. Nu_x and Sh_x distributions versus p at $\lambda=1/3, f_w=0$ *and* $\gamma=1$

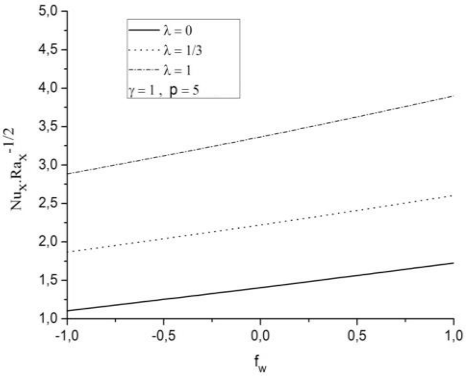

Figure 10. Nu_x distributions versus f_w at $\gamma=1$ *and* $p=5$ *for* $\lambda=(0,1, 1/3)$

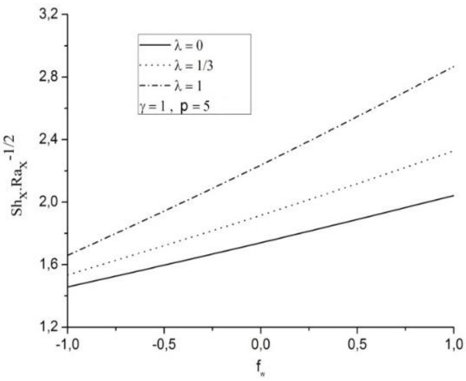

Figure 11. Sh_x distributions versus f_w at $\gamma=1$, $p=5$, *for* $\lambda=(0, 1, 1/3)$

The variation of the heat transfer rate and the mass transfer rate at an impermeable wall, subjected to a uniform heat flux ($\lambda=1/3$) is presented, consecutively, on Figure 8 for different values of γ at $p=2$, and in Figure 9 at $\gamma=1$ for various values of p. From Figure 8 we observe, firstly, that the wall heat and mass transfer rates increase almost linearly in passing from the forced convection to the free convection, on the other hand, the wall heat transfer rate is more significant compared to the wall mass transfer. These two quantities are positive for all selected values of p. From Figure 9, an increase in wall heat and mass transfer rates is noted as p increases. For the values of p less than a critical value ($p=1.76$), the mass transfer rate is predominant. Beyond this value, the trends are reversed.

Figure 10 and Figure 11 show for $\gamma=1$ and $p=5$, respectively, the evolution of the wall heat transfer rate and the wall mass transfer rate as a function of the suction/injection parameter f_w, for three thermal conditions of wall ($\lambda=0$, $\lambda=1$, $\lambda=1/3$). It is very remarkable from these tow graphs that the fluid injection reduces the wall heat and mass transfer rates, while the suction favors them for the three values of λ. In addition, this transfer rates are important for the case where the temperature plate is linearly distributed and less significant for an isothermal plate.

5. CONCLUSION

Thermosolutal mixed convective flow past a vertical wall, immersed in a saturated porous medium with non-uniform permeability has been studied and analyzed in this paper. The studied wall was exposed to different thermal conditions and a lateral fluid suction or injection. The similarity method was used to convert the governing conservation equations into nonlinear ordinary differential equations, which are then numerically solved by the fifth order Runge-Kutta scheme coupled with shooting iteration technique. A graphic presentation and physical interpretations of the obtained results are included. From this study, it was found that free regime convection and high permeability of medium reduce the thicknesses of thermal and concentration boundary layers, involving the intensification of wall heat and mass transfer rates. In addition, for the different wall thermal conditions, the injection of the fluid decreases the wall heat and mass transfer rates, while the suction favors them.

REFERENCES

[1] Nield, D.A., Bejan, A. (2006). Convection in porous media. New York: Springer. https://doi.org/10.1007/0-387-33431-9

[2] Ingham, D.B., Pop, I. (1998). Transport Phenomena in Porous Media I. Pergamon, Oxford. https://doi.org/10.1016/B978-0-08-042843-7.X5000-4

[3] Ingham, D.B., Pop, I. (2002). Transport Phenomena in Porous Media II. Pergamon, Oxford. https://doi.org/10.1016/B978-0-08-043965-5.X5000-4

[4] Vafai, K. (2005). Handbook of porous media, CRC Press. Boca Raton. https://doi.org/10.1201/9780415876384

[5] Murray, B.T., Chen, C.F. (1989). Double-diffusive convection in a porous medium. Journal of Fluid Mechanics, 201: 147-166. http://dx.doi.org/10.1017/S002211208900087X

[6] Postelnicu, A., Pop, I. (1999). Similarity solutions of free convection boundary layers over vertical and horizontal surfaces in porous media with internal heat generation. International Communications in Heat and Mass Transfer, 26(8): 1183-1191. http://dx.doi.org/10.1016/S0735-1933(99)00108-6

[7] Postelnicu, A., Groşan, T., Pop, I. (2000). Free convection boundary-layer over a vertical permeable flat plate in a porous medium with internal heat generation. International Communications in Heat and Mass Transfer, 27(5): 729-738. http://dx.doi.org/10.1016/S0735-1933(00)00153-6

[8] Achemlal, D., Sriti, M., Guedda, M. (2012). Numerical solution of the free convection induced by a heated vertical flat plate embedded in a saturated porous medium with a variable internal heat source. Modell. Meas. Control B, 81: 39-55.

[9] Cortell, R. (2010). Internal heat generation and radiation effects on a certain free convection flow. International Journal of Nonlinear Science, 9(4): 468-479.

[10] Flilihi, E., Sriti, M., Achemlal, D. (2017). Variable heat source and wall radiation effects on boundary layer convection from an inclined plate in non-darcian porous medium. Frontiers in Heat and Mass Transfer (FHMT), 9(1): 1-8. http://dx.doi.org/10.5098/hmt.9.23

[11] Alhumoud J.M. (2019). Non-equilibrium natural convection flow through a porous medium, Mathematical Modelling of Engineering Problems, 6(2): 163-169. https://doi.org/10.18280/mmep.060202

[12] Belhadj, M., Atia, A., Benchatti, A. (2020). Analysis of natural convection in porous media for thermal storage using Darcy-Brinkman-Forcheimer formulation. Mathematical Modelling of Engineering Problems, 7(1): 73-78. https://doi.org/10.18280/mmep.070109

[13] Anghel, M., Takhar, H.S., Pop, I. (2000). Dufour and Soret effects on free convection boundary layer over a vertical surface embedded in a porous medium. Studia Universitatis Babes-Bolyai, Mathematica, 45(4): 11-21.

[14] Postelnicu, A. (2004). Influence of a magnetic field on heat and mass transfer by natural convection from vertical surfaces in porous media considering Soret and Dufour effects. International Journal of Heat and Mass transfer, 47(6-7): 1467-1472. http://dx.doi.org/10.1016/j.ijheatmasstransfer.2003.09.017

[15] Alam, M.S., Rahman, M.M. (2006). Dufour and Soret effects on mixed convection flow past a vertical porous flat plate with variable suction. Nonlinear Analysis: Modelling and Control, 11(1): 3-12. http://dx.doi.org/10.15388/NA.2006.11.1.14761

[16] Postelnicu, A. (2007). Influence of chemical reaction on heat and mass transfer by natural convection from vertical surfaces in porous media considering Soret and Dufour effects. Heat and Mass Transfer, 43(6): 595-602. http://dx.doi.org/10.1007/s00231-006-0132-8

[17] El Haroui, M., Sriti, M., Achemlal, D., Flilihi, E. (2017). Prediction of thermosolutal convection in a porous medium with Soret-Dufour and chemical reaction effects. Computational Thermal Sciences, 9(5): 383-393. http://dx.doi.org/10.1615/ComputThermalScien.2017019817

[18] Harfash, A.J., Meften, G.A. (2019). Couple stresses effect on instability and nonlinear stability in a double diffusive convection. Applied Mathematics and Computation, 341: 301-320. https://doi.org/10.1016/j.amc.2018.08.045

[19] Mahajan, A., Tripathi, V.K. (2021). Effect of nonlinear temperature and concentration profiles on the stability of a layer of fluid with chemical reaction. Canadian Journal of Physics, 99(5): 367-377. https://doi.org/10.1139/cjp-2020-0302

[20] Roblee, L.H.S., Baird, R.M., Tierney, J.W. (1958). Radial porosity variations in packed beds. AIChE Journal, 4(4): 460-464. http://dx.doi.org/10.1002/aic.690040415

[21] Benenati, R.F., Brosilow, C.B. (1962). Void fraction distribution in beds of spheres. AIChE Journal, 8(3): 359-361. http://dx.doi.org/10.1002/aic.690080319

[22] Mohammadein, A.A., El-Shaer, N.A. (2004). Influence of variable permeability on combined free and forced convection flow past a semi-infinite vertical plate in a saturated porous medium. Heat and Mass Transfer, 40(5):

341-346. http://dx.doi.org/10.1007/s00231-003-0430-3
[23] Singh, P.K. (2012). Mixed convection boundary layer flow past a vertical plate in porous medium with viscous dissipation and variable permeability. International Journal of Computer Applications, 48(8): 45-48.
[24] Rees, D.A.S., Pop, I. (2000). Vertical free convection in a porous medium with variable permeability effects. International Journal of Heat and Mass Transfer, 43(14): 2565-2571. http://dx.doi.org/10.5120/7372-0216
[25] El Haroui, M.E., Sriti, M., Achemlal, D. (2015). Double diffusive free convection over a heated vertical plate in a saturated porous medium with soret effect and variable heat source. Modelling, Measurement and Control B, 842015(1).